

Low-frequency excess vibrational modes in two-dimensional glasses

Lijin Wang^{1,*}, Grzegorz Szamel², and Elijah Flenner^{2,†}

¹*School of Physics and Materials Science, Anhui University, Hefei 230601, P. R. China and*

²*Department of Chemistry, Colorado State University, Fort Collins, Colorado 80523, USA*

(Dated: March 5, 2022)

Glasses possess more low-frequency vibrational modes than predicted by Debye theory. These excess modes are crucial for the understanding of the low temperature thermal and mechanical properties of glasses, which differ from those of crystalline solids. Recent simulational studies suggest that the density of the excess modes scales with their frequency ω as ω^4 in two and higher dimensions. Here, we present extensive numerical studies of two-dimensional model glass formers over a large range of glass stabilities. We find that the density of the excess modes follows $D_{\text{exc}}(\omega) \sim \omega^2$ up to around the boson peak, regardless of the glass stability. The stability dependence of the overall scale of $D_{\text{exc}}(\omega)$ correlates with the stability dependence of low-frequency sound attenuation. However, we also find that in small systems, where the first sound mode is pushed to higher frequencies, at frequencies below the first sound mode there are excess modes with a system size independent density of states that scales as ω^3 .

Low-temperature glasses exhibit thermal and mechanical properties [1–7] that distinguish them from low temperature crystalline solids. The low frequency vibrational modes in crystalline solids are plane waves. Their density of states is well described by Debye theory and scales with frequency ω as ω^{d-1} where d is the spatial dimension. For glasses, there are additional low-frequency modes that result in a peak in the reduced total density of states $D(\omega)/\omega^{d-1}$ in d spatial dimensions, which is referred to as the boson peak [8–11]. Understanding the nature of the additional modes provides insight into the physics behind the anomalous properties of glasses and supercooled liquids [12–20].

Mean field theory [21, 22] predicts that the density of the low frequency excess modes $D_{\text{exc}}(\omega)$ grows as ω^β with $\beta = 2$, while several phenomenological models [23–27] predict $\beta = 3$ or 4. Fluctuating elasticity theory [28] predicts that $D_{\text{exc}}(\omega)$ scales as ω^{d+1} , which is the same scaling that the same theory predicts for the sound attenuation coefficient. An analysis based on a fold stability predicts $D_{\text{exc}}(\omega)$ scales as ω^3 in glasses approaching marginal stability [29]. Other recent theories predict the density of the excess modes scales as ω^4 [30–33].

Simulations are a useful tool to examine low-frequency vibrational modes since characteristics of each mode can be investigated, but studying finite systems presents some difficulties. One is that the plane-wave-like modes occur around discrete frequencies, which can be approximated using Debye theory, but the density of states does not exactly follow the Debye prediction. One has to be careful in the calculation of the density of states due to this discrete nature of the plane-wave-like modes [34]. Simulating two-dimensional (2D) glasses adds another potential difficulty since Mermin-Wagner [35–38] fluctuations lead to pronounced finite size effects in some static and dynamic properties of two-dimensional solids.

With increasing system size the glass behaves increasingly as a continuous elastic solid, and it is expected that there are plane-wave-like modes similar to those of Debye theory. This observation has lead researchers to dis-

tinguish between plane-wave-like modes and additional modes. One simple way to do this is to use the participation ratio, which is a measure of how many particles significantly participate in the mode [39, 40]. A more sophisticated approach is to introduce an order parameter that quantifies the similarity between a low-frequency mode in an amorphous solid and a plane wave [40]. Although these two methods are naturally suited for large systems, in principle they can be used for systems of any size. An alternative approach to distinguish modes of different nature is to study small systems in which the first plane-wave-like mode (which is found at a frequency close to the one predicted by Debye theory) is pushed to higher frequencies [41]. The low-frequency modes found in these small systems are postulated to be the modes in excess of the Debye prediction.

Mizuno, Shiba, and Ikeda [40] used the participation ratio and an order parameter to separate modes into extended and excess modes in large, over one-million particle, two- (2D) and three-dimensional (3D) systems. In both dimensions they found that the density of the modes with large participation ratio obeyed Debye scaling. In 3D they found that the density of the excess modes, which they determined are quasi-localized, scales as $D_{\text{loc}}(\omega) \sim \omega^4$.

The scaling of the density of excess modes Mizuno *et al.* found in 3D agrees with the scaling observed previously by studying small systems [41]. Subsequent work by Wang *et al.* [42] confirmed that the picture observed by Mizuno *et al.* in 3D is also found in glasses of various stabilities, up to the stability of laboratory glasses. Numerical simulations have demonstrated overwhelmingly the universality of $D(\omega) \sim \omega^4$ scaling in 3D model glass formers, irrespective of glass preparation protocols, or interaction potentials [40–55]. In their studies of large 2D systems, Mizuno *et al.* found very few low frequency modes with small participation ratio or with small values of plane-wave order parameter. However, the work of Kapteijns, Bouchbinder, and Lerner [56, 57], who studied small systems, found modes below the first plane-wave-

like mode with density scaling as ω^4 . Notably, unlike in higher dimensions, Kapteijns *et al.* found that the pre-factor for the ω^4 scaling grew with system size as $[\log N]^{5/2}$ in 2D. For the much larger system studied by Mizuno *et al.*, it might be expected that there would be a discernible increase in the density of states over the Debye spectrum, but the logarithmic increase with system size would make the increase modest.

In this work, we present results for the density of excess modes, $D_{\text{exc}}(\omega)$, in 2D model glass formers with different interaction potentials and stability. We used two ways to calculate $D_{\text{exc}}(\omega)$. The first method is to subtract off the infinite size system Debye prediction. Except for very low frequencies, this should allow one to examine how the density of modes in excess of the Debye prediction changes with frequency, but the discrete nature of the spectrum at low frequencies makes it hard to determine the low-frequency growth of $D_{\text{exc}}(\omega)$. We used this concept and found that $D_{\text{exc}}(\omega) \sim \omega^2$ in 2D, which differs from previous observations. Importantly, $D_{\text{exc}}(\omega)$ is correlated with the low frequency scaling of sound attenuation, which resembles the correlation we found between the density of the excess modes and the sound attenuation in 3D [19]. To make a more direct connection with previous results we also studied small systems. Unlike previous work, we found a system size and model independent ω^3 scaling of modes far below the first mode predicted by Debye theory. However, these low-frequency modes are very rare even in poorly annealed systems and are absent in our very stable systems.

We performed extensive simulation studies of four 2D model glass formers with spherically symmetric interactions: (I) a system of polydisperse particles interacting via an inverse power law potential $\propto r^{-n}$ (r is the distance of two particles) with $n = 12$ (IPL-12) [58]; (II) a bidisperse system with inverse power law potential with $n = 10$ (IPL-10) [45]; (III) a bidisperse system with Lennard-Jones potential (LJ) [59]; (IV) a bidisperse system with a harmonic potential (HARM) [60]. Details regarding the four models can be found in the Supplemental Material [61].

We created zero-temperature ($T = 0$) glasses by quenching instantaneously equilibrated liquid configurations at parent temperatures T_p to $T = 0$ using the fast inertial relaxation engine [62]. Equilibrated liquids at very high parent temperatures were obtained by performing molecular dynamic simulations using LAMMPS [63]. As discussed elsewhere, glasses obtained using this method are not very stable. To generate stable glasses for the IPL-12 system, we employed the swap Monte Carlo method [64–66] to prepare equilibrated supercooled liquids at low T_p , down to around $37\%T_g$, where $T_g \approx 0.082$ is the estimated experimental glass temperature [58].

The normal modes of $T = 0$ glasses were obtained by diagonalizing the Hessian matrix using ARPACK [67] and Intel Math Kernel Library [68]. The density of states is given by $D(\omega) = \frac{1}{2N-2} \sum_{l=1}^{2N-2} \delta(\omega - \omega_l)$ with ω_l the frequency of mode l and N the number of particles. In

glasses, there are no pure plane-wave modes and the frequencies of the plane-wave-like modes are generally clustered around the Debye predictions [34, 69]. Since Debye theory predicts discrete modes in finite systems, one has to be careful when calculating the density of states since that calculation requires a division by the bin size $\delta\omega$. If $\delta\omega$ is not chosen correctly, the density is inaccurate. The calculation of the cumulative density of states $I(\omega) = \int_0^\omega D(\omega')d\omega'$ does not suffer from this issue since it amounts to counting the number of states up to ω and dividing by the total number of states. For this reason, we focus on the cumulative density of states $I(\omega)$.

To obtain the excess modes Mizuno and coworkers [40] defined a threshold of the participation ratio $P_c = 0.01$ to divide plane-wave-like modes and quasi-localized modes. They concluded that there are few to no low-frequency quasi-localized modes in poorly annealed 2D glasses [40]. Additionally, the Debye theory accurately predicted the low-frequency density of states, but there was still a boson peak at higher frequencies. We attempted to use the participation ratio to separate the modes, but we found that the scaling behavior of the excess modes in 2D stable IPL-12 model glasses depends strongly on the choice of P_c . This strong dependence makes it impossible to determine the scaling of $I(\omega)$ using the participation ratio. Therefore, we utilized a different procedure by subtracting from the cumulative density of states the Debye prediction [28]

$$I_{\text{exc}}(\omega) = I(\omega) - I_D(\omega), \quad (1)$$

where $I(\omega)$ is the cumulative density of states of all modes and $I_D(\omega)$ is the Debye prediction [70], $I_D(\omega) = A_D\omega^d/d$ with Debye level A_D determined independently from mechanical moduli [70]. We note that this procedure does not take into account that the mode frequencies are discrete for finite systems.

Figure 1(a) shows excess cumulative density of states $I_{\text{exc}}(\omega)$ for our 2D IPL-12 model glasses for $N = 20000$ at different parent temperatures T_p . The glass stability increases with decreasing T_p [42, 48, 58]. We use parent temperatures ranging from $T_p = 0.400$, which is above the onset temperature of slow dynamics $T_o = 0.250$, down to $T_p = 0.030$, which is below the estimated laboratory glass temperature $T_g = 0.082$ [58]. For the lowest frequencies where we can clearly estimate a power law, we find that $I_{\text{exc}}(\omega)$ scales as ω^3 , $I_{\text{exc}}(\omega) \simeq A_2\omega^3/3$, which suggests that $D_{\text{exc}}(\omega) \simeq A_2\omega^2$. We find that this scaling continues up to around the Ioffe-Regal limit, which is around the boson peak frequency [10], irrespective of the glass's stability, see Fig. 1(b). We find that the coefficient quantifying the magnitude of the excess modes density, A_2 , is stability-dependent. A_2 is nearly constant for larger T_p , but decreases by a factor of 13 for our lowest T_p . This indicates that there are fewer excess modes for increasingly stable 2D glasses, which is consistent with observations for 3D glasses [42, 48, 55].

Previous work [18, 19, 28] found a connection between

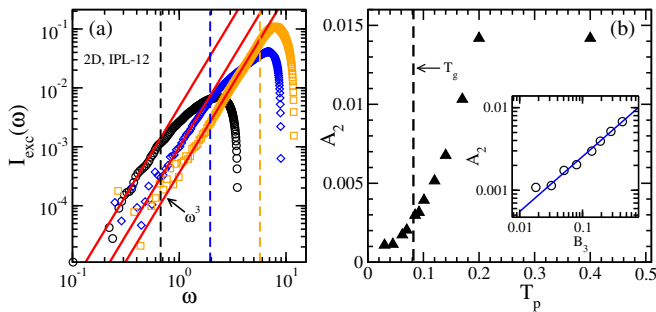


FIG. 1: (color online) (a) Cumulative density of states of excess modes $I_{\text{exc}}(\omega) = I(\omega) - I_D(\omega)$ at $T_p = 0.400$ (circles), 0.085 (diamonds), and 0.030 (squares) in $N = 20000$ system in the 2D IPL-12 model. $I(\omega)$ is the total cumulative density of states while $I_D(\omega) = 1/2 A_D \omega^2$ with A_D Debye level. The red lines are fits to $I_{\text{exc}}(\omega) = 1/3 A_2 \omega^3$ while vertical lines indicate boson peak frequencies. (b) T_p dependence of A_2 , with the estimated glass transition temperature T_g indicated for reference. Glass stability increases with decreasing T_p . (Inset) A_2 against the pre-factor B_3 in $\Gamma(\omega) = B_3 \omega^3$ with Γ the transverse sound attenuation coefficient. Details for the calculation of Γ can be found in Ref.[19]. The blue line indicates a fit to $A_2 \sim B_3^\gamma$ with $\gamma \approx 2/3$.

sound attenuation and density of states of excess low-frequency modes. Inspired by this work we examined whether $I_{\text{exc}}(\omega)$ is related to sound attenuation in 2D. The frequency dependence of the transverse sound attenuation coefficient $\Gamma(\omega)$ in 2D glasses follows the Rayleigh scattering scaling as $\Gamma(\omega) = B_3 \omega^3$ and B_3 decreases with increasing glass stability [18]. Here, we study the relation between B_3 and A_2 , see the inset to Fig. 1b. We find $A_2 \sim B_3^\gamma$ with $\gamma \approx 2/3$, and thus we establish that in 2D the excess modes density is related to sound attenuation, which is consistent with our result for 3D glasses.

Since the method introduced in this Letter is different from methods used before by us and others, we checked what results it produces if used for 3D glasses where it has been firmly established that $I_{\text{exc}}(\omega) \sim \omega^5$. In Fig. 2 we show $I_{\text{exc}}(\omega)$ in 3D IPL-12 glasses for two stabilities, a very poorly annealed glass with $T_p = 0.200$ and a very stable glass with $T_p = 0.062$. These are the same glasses examined in Ref. [42]. We find that $I_{\text{exc}}(\omega) \sim \omega^5$ up to a frequency close to the boson peak for both glasses, which indicates the resulting scaling of $I_{\text{exc}}(\omega)$ determined using Eq. 1 is consistent with that of $I_{\text{exc}}(\omega)$ calculated with previously used procedures [40, 42, 44]. Additionally, these results suggest that in 3D the end of the ω^5 scaling of $I_{\text{exc}}(\omega)$, ω_g , is around the boson peak frequency. We note that our procedure cannot be used for frequencies below the lowest frequency plane wave mode predicted by the Debye theory. More importantly, it will only reveal the proper scaling if there is a near continuum of modes [34].

Debye theory predicts that the lowest normal mode frequency increases with decreasing N . It has been argued that the scaling of the excess modes could be obtained

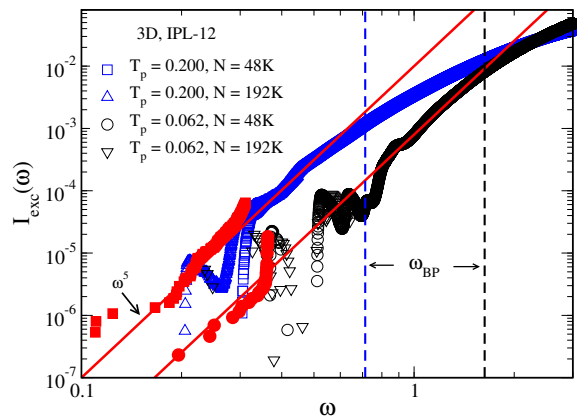


FIG. 2: (color online) Cumulative density of states of excess modes $I_{\text{exc}}(\omega) = I(\omega) - I_D(\omega)$ in the 3D IPL-12 model glasses, with the boson peak frequency indicated. $I(\omega)$ is the total cumulative density of states and $I_D(\omega) = A_D \omega^3/3$ with A_D being the Debye level. Red filled squares and circles represent $I(\omega)$ at frequencies below around the first Debye frequency at $T_p = 0.200$ and $T_p = 0.062$, respectively, in the $N = 48000$ system. The red lines correspond to $I_{\text{exc}}(\omega) \sim \omega^5$.

from the low frequency density of states for small systems since the frequency of the plane-wave-like modes is pushed to high frequencies. Using this reasoning, $I_{\text{exc}}(\omega)$ can be determined by calculating the total cumulative density of states $I(\omega)$ for frequencies below the first predicted Debye mode frequency. One may expect $I(\omega) = I_{\text{exc}}(\omega)$ for low frequencies if the excess modes were independent of the plane-wave like modes, which we found for 3D glasses with different stabilities, see Fig. 2. The low-frequency tail of $I(\omega)$ is well described by a power law $I_{\text{exc}}(\omega) \sim \omega^5$ for $T_p = 0.200$ and $T_p = 0.062$. However, in 2D glasses much below the first Debye frequency we find $I(\omega) \sim \omega^4$, which suggests that $D_{\text{exc}}(\omega) \sim \omega^3$. Previous studies reported $D_{\text{exc}}(\omega) \sim \omega^4$ [56, 57], which would imply that $I_{\text{exc}}(\omega) \sim \omega^5$. To make sure this observation is model independent, we calculated $I(\omega)$ for small systems at frequencies much lower than the first Debye frequency in different models of glass formers.

In Fig. 3 we show the total cumulative density of states $I(\omega)$ for $N = 3000$ system in the 2D IPL-12 model. There is a range of frequencies below the lowest Debye mode frequency (≈ 0.261) that is well described by $I(\omega) \sim \omega^4$. To check the quartic scaling, we examined $I(\omega)/\omega^4$, which is shown in the inset to Fig. 3, and we find that there is a low-frequency plateau. Previous results suggest that $I(\omega) \sim \omega^5$ at frequencies much below the first Debye mode in 2D glasses [56, 57], and that $I(\omega)$ should be system size dependent. However, we find that the ω^5 scaling is only valid for an intermediate-frequency regime below the peak of $I(\omega)$, and appears to be only a transition between the low frequency scaling and the change of the scaling due to the emergence of plane-wave-like modes. We also find that $I(\omega)$ is system size independent at frequencies much lower than the first frequency predicted

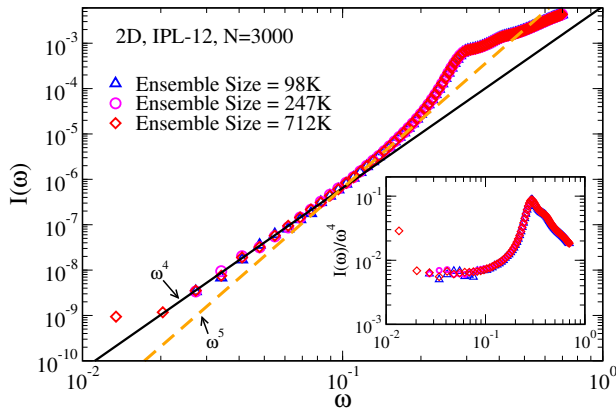


FIG. 3: (color online) The total cumulative density of states $I(\omega)$ for $N = 3000$ system at $T_p = 0.400$ with different ensemble sizes in the 2D IPL-12 model. The solid and dashed lines represent power laws of ω^4 and ω^5 respectively. For reference, the lowest Debye mode frequency is about 0.261. (Inset) The same data plotted as $I(\omega)/\omega^4$ vs. ω .

by Debye theory.

There are very few modes that contribute to the low frequency ω^4 scaling of $I(\omega)$ for our least stable 2D glass. For example, on average there is only one mode lying in the low-frequency $I(\omega) \sim \omega^4$ regime every one hundred configurations for the $N = 3000$ system. The lower the frequency we want to examine, the larger the ensemble size N_{En} (number of configurations) we need. However, we do not observe N_{En} dependence of the quartic scaling regime in $N = 3000$ system when N_{En} ranges from around 0.1 million to our maximum 0.71 million examined, see Fig. 3. The same conclusion can also be drawn in our study of the $N = 1000$ system where the maximum N_{En} is around 2.2 million [61]. In addition, we checked that the previously reported ω^5 scaling in some systems is due to ensemble size not being large enough, which hinders the observation of the ω^4 scaling at much lower frequencies. We also find that the ω^5 scaling regime vanishes for very small systems, Fig. 4. Since the number of these low-frequency modes decreases with increasing stability, we could not examine the stability dependence of these modes. However, we do not exclude the possibility that thermal relaxation can change the scaling of these low-frequency modes [54].

We find that this low-frequency quartic scaling of $I(\omega)$ in 2D is universal, *i.e.* it does not depend on the model glass former, see Fig. 4. In addition, there are common features shared by each model. First, the pre-factor of the quartic scaling does not depend on system size. This conclusion is different than the conclusion of Ref. [56], namely that $I_{exc}(\omega) = A_4\omega^5/5$ and the pre-factor A_4 grows as $(\log N)^{5/2}$, *i.e.* there should be more excess modes in a larger system. Second, the low-frequency scaling $I(\omega) \sim \omega^4$ works up to a larger frequency with decreasing system size. It deserves further study to check whether the upper frequency for this scaling corre-

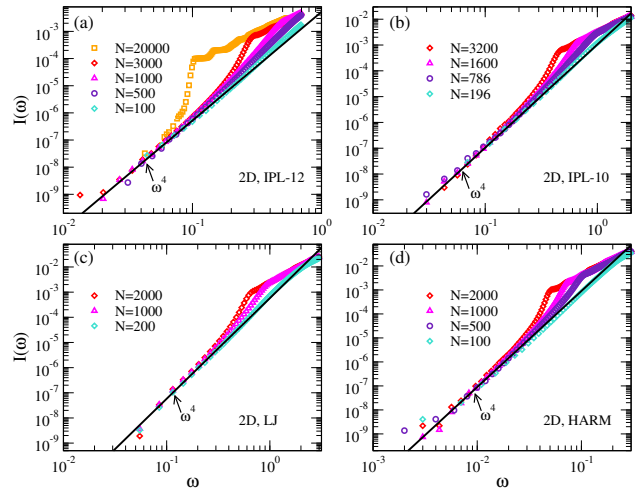


FIG. 4: (color online) The total cumulative density of states $I(\omega)$ for different system sizes in (a) the 2D IPL-12 model, (b) 2D IPL-10 model, (c) 2D LJ model and (d) 2D HARM model. In each panel, the solid line corresponds to the power law of ω^4 and represents the low frequency data very well for all model glass formers examined. We plotted the same data as $I(\omega)/\omega^4$ against ω in the Supplemental Material [61].

lates with any known characteristic frequency. Figures 3 and 4, therefore, demonstrate that $I(\omega) \sim \omega^4$ at frequencies much lower than the first frequency predicted by Debye theory in 2D glasses and the pre-factor for this power law shows no system size dependence.

We utilized two methods to examine the excess density of states in 2D glasses. In large systems, we find evidence that the excess density of states scale as ω^2 . We find that the pre-factor A_2 of this scaling law correlates with the sound attenuation coefficient. However, in small systems, where the frequencies of plane-wave-like modes are pushed higher, we find that the modes below the lowest Debye frequency have density of states scaling as ω^3 , with a system size-independent pre-factor. This inconsistent behavior is not found in 3D glasses using the same analysis.

Our results leave several open questions. First, why is the scaling of excess modes different above and below the first mode predicted by Debye theory? One possibility is that our systems are not large enough to accurately determine $I_{exc}(\omega)$ by subtracting off the Debye contribution at low frequencies. However, we do find an overlapping frequency range where we find that the excess density of states scales as ω^2 when we subtract off the Debye contribution and where the excess density of states scales as ω^3 for very small systems, see Fig. 3 of the Supplemental Material [61]. Thus, it seems that the presence of plane waves influences the scaling of the excess density of states in 2D glasses.

There may also be a gap in the excess density of states and the ω^2 and the ω^3 scaling does not extend to $\omega = 0$, which would be consistent with the conclusions of Ref. [40]. It is very difficult to numerically test these

possibilities with the current computer power since the ω^2 and ω^3 scaling represents very few modes at small ω . Future related theoretical work may shed some light on this issue.

Third, why is the excess density of states different from that of 3D glasses? Fluctuation elasticity theories predict that $D_{\text{exc}}(\omega)$ depends on spatial dimension as ω^{d+1} [28]. Thus, the predicted $D_{\text{exc}}(\omega) \sim \omega^4$ in 3D glasses is consistent with 3D numerical observations. The predicted scaling of $D_{\text{exc}}(\omega) \sim \omega^3$ of 2D glasses is consistent with what we find in small systems. However, it has been shown that $D_{\text{exc}}(\omega) \sim \omega^4$ in 2D glasses [56] in contrast to the fluctuating elasticity theory prediction. We notice that the dynamics of 2D and 3D glass-forming liquids was reported to be fundamentally different [35]. It may be also interesting to probe whether there is any connection between the difference in dynamics between 2D and 3D glass-forming liquids and the difference in the density

of states of excess modes between 2D and 3D glasses.

Finally, it is possible that the upper frequency cutoff of the low frequency scaling, ω_g , is below the frequency range where we found ω^2 scaling of $D_{\text{exc}}(\omega)$ in large 2D glasses. If this were the case, it would differ from our finding in 3D that ω_g is around the boson peak frequency. We leave it for future work to examine what determines ω_g and if it depends on dimension.

We wish to thank Andrea Ninarello for generously providing equilibrated configurations at very low parent temperatures and E. Lerner for comments on the manuscript. L. W. acknowledges the support from National Natural Science Foundation of China (No. 12004001), Anhui Province (No. S020218016), Hefei City (No. Z020132009), and Anhui University (Startup fund). E.F. and G.S. acknowledge the support from NSF Grant CHE-1800282.

* lijn.wang@ahu.edu.cn

† flenner@gmail.com

- [1] R. C. Zeller and R. O. Pohl, *Phys. Rev. B* **4**, 2029 (1971).
- [2] P. W. Anderson, B. I. Halperin and C. M. Varma, *Philos. Mag.*, **25**, 1 (1972).
- [3] W. A. Phillips, *J. Low Temp. Phys.* **7**, 351 (1972).
- [4] M. P. Zaitlin and A. C. Anderson, *Phys. Rev. B: Solid State*, **12**, 4475 (1975).
- [5] R. O. Pohl, X. Liu and E. Thompson, *Rev. Mod. Phys.*, **74**, 991 (2002).
- [6] M. Ozawa, L. Berthier, G. Biroli, A. Rosso and G. Tarjus, *Proc. Natl. Acad. Sci. U.S.A.* **115**, 6656 (2018).
- [7] J. Ketkaew, W. Chen, H. Wang, A. Datye, M. Fan, G. Pereira, U. D. Schwarz, Z. Liu, R. Yamada, W. Dmowski, M. D. Shattuck, C. S. O'Hern, T. Egami, E. Bouchbinder and J. Schroers, *Nat. Commun.* **9**, 3271 (2018).
- [8] T. S. Grigera, V. Martin-Mayor, G. Parisi, and P. Verrocchio, *Nature (London)* **422**, 289 (2003).
- [9] K. Inoue, T. Kanaya, S. Ikeda, K. Kaji, K. Shibata, M. Misawa, and Y. Kiyonagi, *J. Chem. Phys.* **95**, 195332 (1991).
- [10] H. Shintani and H. Tanaka, *Nat. Mater.* **7**, 870 (2008).
- [11] U. Buchenau, A. Wischniewski, M. Ohl, and E. Fabiani, *J. Phys.: Condens. Matter* **19**, 205106 (2007).
- [12] K. Chen, M. L. Manning, P. J. Yunker, W. G. Ellenbroek, Z. X. Zhang, A. J. Liu, and A. G. Yodh, *Phys. Rev. Lett.* **107**, 108301 (2011).
- [13] A. Widmer-Cooper, H. Perry, P. Harrowell, and D. R. Reichman, *Nat. Phys.* **4**, 711 (2008).
- [14] S. S. Schoenholz, A. J. Liu, R. A. Riggleman, and J. Rottler, *Phys. Rev. X* **4**, 031014 (2014).
- [15] M. L. Manning and A. J. Liu, *Phys. Rev. Lett.* **107**, 108302 (2011).
- [16] J. Zylberg, E. Lerner, E. Y. Bar-Sinai and E. Bouchbinder, *Proc. Natl. Acad. Sci. U.S.A.* **114**, 7289 (2017).
- [17] E. Flenner, L. Wang and G. Szamel, *Soft Matter*, **16**, 775 (2020).
- [18] A. Moriel, G. Kapteijns, C. Rainone, J. Zylberg, E. Lerner and E. Bouchbinder, *J. Chem. Phys.*, **151**, 104503 (2019).
- [19] L. Wang, L. Berthier, E. Flenner, P. Guan and G. Szamel, *Soft Matter*, **15**, 7018 (2019).
- [20] N. Xu, V. Vitelli, A. J. Liu and S. R. Nagel, *Europhys. Lett.*, **90**, 56001 (2010).
- [21] E. DeGiuli, A. Laversanne-Finot, G. Düring, E. Lerner, and M. Wyart, *Soft matter* **10**, 5628 (2014).
- [22] S. Franz, G. Parisi, P. Urbani, and F. Zamponi, *Proc. Nat. Acad. Sci. USA* **112**, 14539 (2015).
- [23] U. Buchenau, Yu. M. Galperin, V. L. Gurevich, and H. R. Schober, *Phys. Rev. B* **43**, 5309 (1991).
- [24] H. R. Schober and C. Oligschleger, *Phys. Rev. B* **53**, 11469 (1996).
- [25] V. L. Gurevich, D. A. Parshin, and H. R. Schober, *Phys. Rev. B* **67**, 094203 (2003).
- [26] V. Gurarie and J. T. Chalker, *Phys. Rev. B* **68**, 134207 (2003).
- [27] A. Kumar, I. Procaccia, and M. Singh, arXiv:2102.12368 (2021).
- [28] W. Schirmacher, G. Ruocco, and T. Scopigno, *Phys. Rev. Lett.* **98**, 025501 (2007).
- [29] N. Xu, A. Liu, and S. R. Nagel, *Phys. Rev. Lett.* **119**, 215502 (2017).
- [30] H. Ikeda, *Phys. Rev. E* **99**, 050901(R) (2019).
- [31] E. Stanifer, P. K. Morse, A. A. Middleton, and M. L. Manning, *Phys. Rev. E* **98**, 042908 (2018).
- [32] E. Bouchbinder, E. Lerner, C. Rainone, P. Urbani, and F. Zamponi, arXiv:2012.11558 (2020).
- [33] W. Ji, M. Popović, T. W. J. de Geus, E. Lerner, and M. Wyart, *Phys. Rev. E* **99**, 023003 (2019).
- [34] E. Bouchbinder and E. Lerner, *New J. Phys.* **20**, 073022 (2018).
- [35] E. Flenner and G. Szamel, *Nature Commun.* **6**, 7392 (2015).
- [36] S. Vivek, C.P. Kelleher, P.M. Chaikin, and E.R. Weeks, *Proc. Natl. Acad. Sci. USA* **114**, 1850 (2017).
- [37] B. Illing, S. Fritschi, H. Kaiser, C.L. Klix, G. Maret, and P. Keim, *Proc. Natl. Acad. Sci. USA* **114**, 1856 (2017).
- [38] E. Flenner and G. Szamel, *Proc. Natl. Acad. Sci. USA* **116**, 2015 (2018).

- [39] V. Mazzacurati, G. Ruocco, M. Sampoli, *Europhys. Lett.* **34**, 681 (1996).
- [40] H. Mizuno, H. Shiba, and A. Ikeda, *Proc. Natl. Acad. Sci. U.S.A.* **114**, E9767 (2017).
- [41] E. Lerner, G. Düring, and E. Bouchbinder, *Phys. Rev. Lett.* **117**, 035501 (2016).
- [42] L. Wang, A. Ninarello, P. Guan, L. Berthier, G. Szamel and E. Flenner, *Nat. Commun.* 2019, **10**, 26.
- [43] M. Baity-Jesi, V. Martić-Mayor, G. Parisi, and S. Perez-Gaviro, *Phys. Rev. Lett.* **115**, 267205 (2015).
- [44] M. Shimada, H. Mizuno, and A. Ikeda, *Phys. Rev. E* **97**, 022609 (2018).
- [45] G. Kapteijns, E. Bouchbinder, and E. Lerner, *J. Chem. Phys.* **148**, 214502 (2018).
- [46] E. Lerner, *Phys. Rev. E* **101**, 032120 (2020).
- [47] L. Angelani, M. Paoluzzi, G. Parisi and G. Ruocco, *Proc. Natl. Acad. Sci. USA*, 2018, **115**, 8700.
- [48] C. Rainone, E. Bouchbinder, and E. Lerner, *Proc. Natl. Acad. Sci. USA*, 2020, **117**, 5228.
- [49] S. Bonfanti, R. Guerra, C. Mondal, I. Procaccia, and S. Zapperi, *Phys. Rev. Lett.* **125**, 085501 (2020).
- [50] K. G. Lopez, D. Richard, G. Kapteijns, R. Pater, T. Vaknin, E. Bouchbinder, and E. Lerner, *Phys. Rev. Lett.* **125**, 085502 (2020).
- [51] M. Shimada, H. Mizuno, L. Berthier, and A. Ikeda, *Phys. Rev. E* **101**, 052906 (2020).
- [52] P. Das and I. Procaccia, *Phys. Rev. Lett.* **126**, 085502 (2021).
- [53] M. Shimada, H. Mizuno, M. Wyart, and A. Ikeda, *Phys. Rev. E* **98**, 060901(R) (2018).
- [54] E. Lerner and E. Bouchbinder, *Phys. Rev. E* **96**, 020104(R) (2017).
- [55] W. Ji, T. W. J. de Geus, M. Popović, E. Agoritsas, and M. Wyart, *Phys. Rev. E* **102**, 062110 (2020).
- [56] G. Kapteijns, E. Bouchbinder and E. Lerner, *Phys. Rev. Lett.*, 2018, **121**, 055501.
- [57] V. V. Krishnan, K. Ramola, and S. Karmakar, arXiv:2014.0918 (2021).
- [58] L. Berthier, P. Charbonneau, A. Ninarello, M. Ozawa, and S. Yaida, *Nat. Commun.* **10**, 1508 (2019).
- [59] R. Bruning, D. A. St-Onge, S. Patterson, and W. Kob, *J. Phys.: Condens. Matter* **21**, 035117 (2009).
- [60] C. S. O'Hern, L. E. Silbert, A. J. Liu, and S. R. Nagel, *Phys. Rev. E* **68**, 011306 (2003).
- [61] See Supplemental Material at * for simulation details of the four interaction potential models and more supporting analysis.
- [62] E. Bitzek, P. Koskinen, F. Gähler, M. Moseler, and P. Gumbsch, *Phys. Rev. Lett.* **97**, 170201 (2006).
- [63] S. Plimpton, *J. Comput. Phys.* **117**, 1 (1995).
- [64] T. S. Grigera and G. Parisi, *Phys. Rev. E: Stat., Nonlinear, Soft Matter Phys.* **63**, 045102(R) (2001).
- [65] A. Ninarello, L. Berthier, and D. Coslovich, *Phys. Rev. X* **7**, 021039 (2017).
- [66] L. Berthier, D. Coslovich, A. Ninarello, and M. Ozawa, *Phys. Rev. Lett.* **116**, 238002 (2016).
- [67] <http://www.caam.rice.edu/software/ARPACK/>.
- [68] <https://software.intel.com/en-us/mkl/>.
- [69] G. Kapteijns, E. Bouchbinder and E. Lerner, arXiv:2106.12613.
- [70] C. Kittel, *Introduction to Solid State Physics*, 7th Ed. (Wiley, New York, 1996). (Wiley, New York, 1996).
-

Supplemental Material: Low-frequency excess vibrational modes in two-dimensional glasses

Lijin Wang¹, Grzegorz Szamel², and Elijah Flenner²

¹*School of Physics and Materials Science, Anhui University, Hefei 230601, P. R. China and*

²*Department of Chemistry, Colorado State University, Fort Collins, Colorado 80523, USA*

In the supplemental material, we first describe the simulation details of the four model glass formers where we produce results presented in the main text, and then show further results to support some of our descriptions in the main text.

I. SIMULATIONS

Our each simulated 2D model is composed of N discs with equal mass m . Periodic boundary conditions are applied in all directions in all model glasses examined.

Our IPL-12 model and IPL-10 model are the purely repulsive inverse power law potential models with different simulation parameters, and hence we describe the two models together. In the inverse power law potential, the interaction between two particles i and j with the separation r_{ij} is given by $V_{IPL}(r_{ij}) = \left[\left(\frac{\sigma_{ij}}{r_{ij}}\right)^n + c_0 + c_2 \left(\frac{r_{ij}}{\sigma_{ij}}\right)^2 + c_4 \left(\frac{r_{ij}}{\sigma_{ij}}\right)^4\right]H(r_{ij}^c - r_{ij})$, where $H(r)$ is the Heaviside step function, and the constants c_0 , c_2 and c_4 are chosen to make $V(r_{ij})$ and its first and second derivatives continuous at the interaction cutoff r_{ij}^c .

In our 2D *IPL-12 model* [1], the exponent $n = 12$ in $V_{IPL}(r_{ij})$ and the interaction cutoff $r_{ij}^c = 1.25\sigma_{ij}$. We use a continuous size polydispersity with the probability distribution of particle diameters $\sigma \in [0.73, 1.62]$ following $F(\sigma) \sim \frac{1}{\sigma^3}$; the cross-diameter σ_{ij} obeys a non-additive mixing rule, $\sigma_{ij} = \frac{\sigma_i + \sigma_j}{2}(1 - \lambda|\sigma_i - \sigma_j|)$ with $\lambda = 0.2$. We performed simulations in this model system at the number density $\rho = 1.0$ and different parent temperatures T_p ranging from $T_p = 0.400$ to $T_p = 0.030$.

In our 2D *IPL-10 model* [2], $n = 10$ in $V_{IPL}(r_{ij})$ and $r_{ij}^c = 1.48\sigma_{ij}$. This model system is composed of a 50:50 binary mixture of A discs and B discs. Here, we set $\sigma_{AA} = 1.0$, $\sigma_{BB} = 1.4$, and $\sigma_{AB} = 1.18$. High-temperature equilibrated configurations in this model were created at $T_p = 2.0$ and $\rho = 0.86$.

Our 2D *LJ-12 model* [3] is the Lennard-Jones potential system filled with two types of discs: A discs and B discs. The number ratio of A discs to B disc is 65 : 35. The interaction between two discs i and j is $V_{LJ}(r_{ij}) = [f(r_{ij}) - f(r_{ij}^c) - (r_{ij} - r_{ij}^c)f'(r_{ij}^c)]H(r_{ij}^c - r_{ij})$, where $f(r_{ij}) = 4\epsilon_{ij}\left[\left(\frac{\sigma_{ij}}{r_{ij}}\right)^{12} - \left(\frac{\sigma_{ij}}{r_{ij}}\right)^6\right]$, $H(r)$ is the Heaviside step function, and $r_{ij}^c = 2.5\sigma_{ij}$. Here, $\sigma_{AA} = 1.0$, $\sigma_{BB} = 0.88$, $\sigma_{AB} = 0.8$, $\epsilon_{AA} = 1.0$, $\epsilon_{BB} = 0.5$, and $\epsilon_{AB} = 1.5$. Our equilibrated configurations in this model system were obtained at $T_p = 6.0$ and $\rho = 1.2$.

In our 2D *HARM model*, the interaction between two particles i and j is the purely repulsive harmonic potential $V_{HARM}(r_{ij}) = (1 - r_{ij}/\sigma_{ij})^2/2$ when their separation r_{ij} is smaller than $\sigma_{ij} = 0.5(\sigma_i + \sigma_j)$, and zero otherwise. Our model system is composed of a 50:50 binary mixture of A and B discs. Here, $\sigma_A = 1.4$ and $\sigma_B = 1.0$. We got equilibrated configurations in this model system at $T_p = 0.1$ and $\rho = 0.946$.

II. FURTHER RESULTS

In Fig. 1 we show the ensemble size dependence of the total cumulative density of states $I(\omega)$ in the 2D IPL-12 model system with $N = 1000$. For the same data, we also show the plot of $I(\omega)/\omega^4$ vs. ω in the inset. Our maximum ensemble size in this system is around 2.2 million. It can be seen the results do not depend on ensemble size examined here.

Figure 2 shows $I(\omega)/\omega^4$ and $I(\omega)/\omega^5$ against ω for the same data as presented in Fig.3 in the main text. An approximate plateau in the $I(\omega)/\omega^4$ plot but not $I(\omega)/\omega^5$ plot at very low frequencies in each model can be observed, further suggesting $I(\omega) \sim \omega^4$ should be the correct scaling.

Figure 3 demonstrates that there is an overlapping frequency region where the ω^3 scaling is followed by the cumulative density of excess modes $I_{\text{exc}}(\omega)$ determined by subtracting off the Debye contribution and where the ω^4 scaling is followed by the cumulative density of all modes in very small systems.

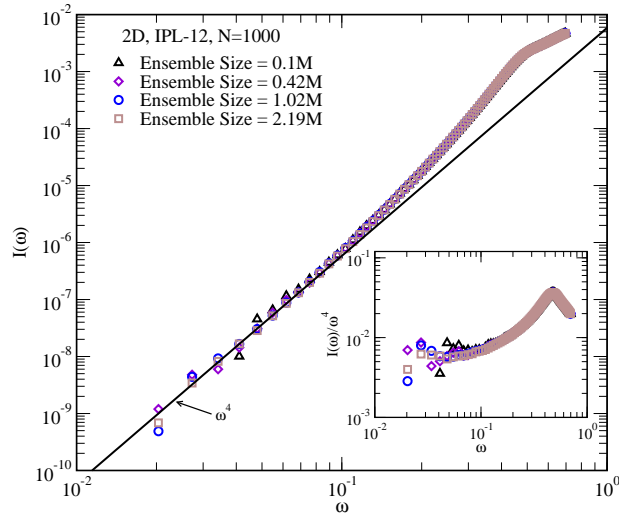


FIG. 1: Ensemble size dependence of the total cumulative density of states $I(\omega)$ at $T_p = 0.400$ for $N = 1000$ system in the 2D IPL-12 model. The solid line represents $I(\omega) \sim \omega^4$. (Inset) The same data plotted as $I(\omega)/\omega^4$ against ω .

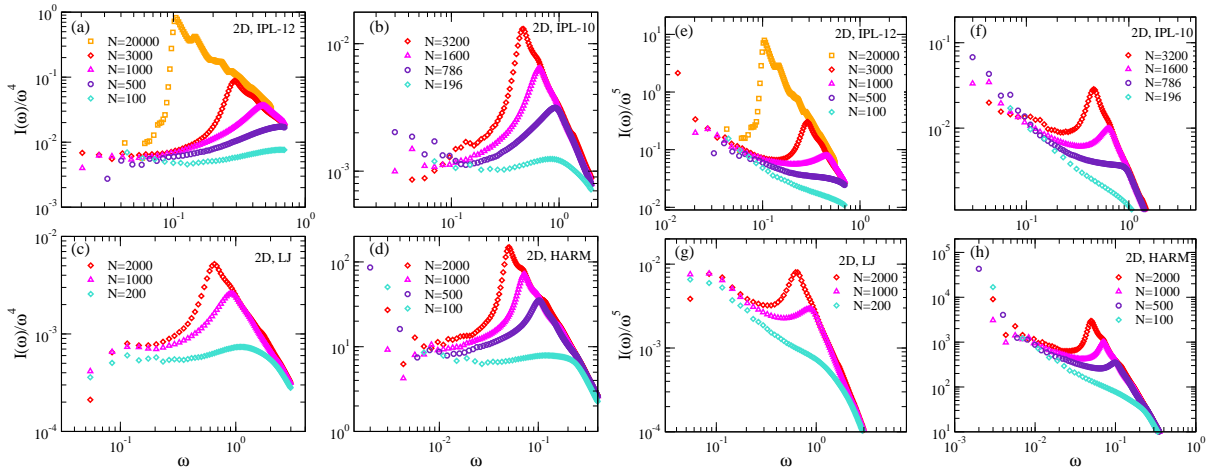


FIG. 2: The reduced total cumulative density of states $I(\omega)/\omega^4$ and $I(\omega)/\omega^5$ in small systems in the 2D IPL-12 model [(a) and (e)], 2D IPL-10 model [(b) and (f)], 2D LJ model [(c) and (g)], and 2D HARM model [(d) and (h)].

-
- [1] L. Berthier, P. Charbonneau, A. Ninarello, M. Ozawa, and S. Yaida, Nat. Commun. **10**, 1508 (2020).
[2] G. Kapteijns, E. Bouchbinder, and E. Lerner, J. Chem. Phys. **148**, 214502 (2018).
[3] R. Bruning, D. A. St-Onge, S. Patterson, and W. Kob, J. Phys.: Condens. Matter **21**, 035117 (2009).
[4] C. S. O'Hern, L. E. Silbert, A. J. Liu, and S. R. Nagel, Phys. Rev. E **68**, 011306 (2003).

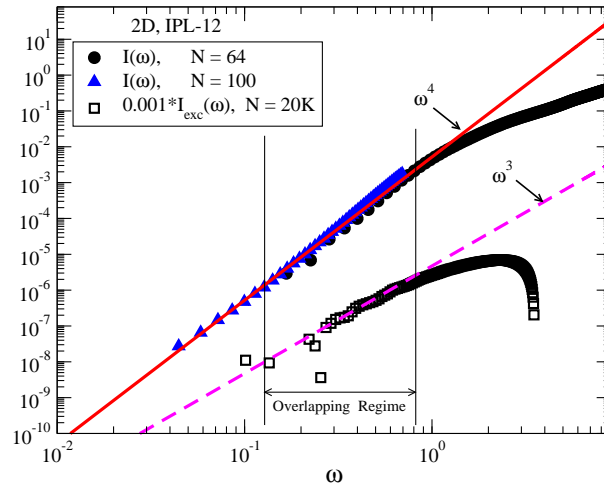


FIG. 3: Comparison of the cumulative density of states of excess modes $I_{\text{exc}}(\omega)$ calculated by subtracting off the Debye contribution (see Eq.1 in the main text) in $N = 20000$ system and the total cumulative density of states $I(\omega)$ in $N = 64$ and 100 systems at $T_p = 0.400$ in the 2D IPL-12 model. Dashed and solid lines correspond to $I_{\text{exc}}(\omega) \sim \omega^3$ and $I(\omega) \sim \omega^4$, respectively. One can see there is an overlapping frequency range (indicated by the horizontal line with arrows in both ends) where $I_{\text{exc}}(\omega)$ scales as ω^3 and where $I(\omega)$ scales as ω^4 . $I_{\text{exc}}(\omega)$ is rescaled by a factor of 0.001 for visualization purpose.

